

PHOTOCATALYSIS OF  
GLYCEROL SOLUTION

ANG CHUN HOW

THESIS SUBMITTED IN FULLFILMENT OF THE REQUIREMENTS FOR THE  
DEGREE OF BACHELOR OF CHEMICAL ENGINEERING

FACULTY CHEMICAL ENGINEERING & NATURAL RESOURCES  
UNIVERSITI MALAYSIA PAHANG

2013

## ABSTRACT

Several papers have addressed the production of  $H_2$  from glycerol solution using catalyst. One of the most innovative ways is via photocatalysis. In this study, titania act as the base catalyst on which copper dopant varies the physicochemical properties. Ultimately, this work was aimed to synthesized and investigated the physicochemical properties of titania supported copper,  $(Cu/TiO_2)$  photocatalyst for photoreaction of glycerol solution. The photocatalyst,  $Cu/TiO_2$  was prepared via wet impregnation method with doped 2, 5, 10, 15, 20 and 25 wt% of Cu. X-ray fluorescence (XRF) showed that the composition of Cu followed the doped weight percentage on  $TiO_2$  and liquid-nitrogen physisorption showed that the BET specific surface area decreased with the increment of Cu loading. Thermogravimetric analysis (TGA) showed that Cu decomposed around 450 to 550 K while X-ray diffraction (XRD) proved the  $Cu/TiO_2$  was anatase with a new peak  $2\theta = 13^\circ$  found as the appearance peak of CuO species. The measured densities were differed from the theoretical calculated densities. The photoreactivity of  $Cu/TiO_2$  was tested with methylene blue decomposition and the results have indicated that  $Cu/TiO_2$  possessed photoreactivity. The conversions for all the photocatalysts with Cu loading were higher than the pristine  $TiO_2$ . This has confirmed that Cu loading has effectively increased the photoreaction of glycerol solution. The 2 wt%  $Cu/TiO_2$  photocatalyst showed the highest conversion at 97.78%. However, the conversion shows decreasing trend with the increment of Cu loading except for 25 wt%  $Cu/TiO_2$ . The concentration profiles were fitted to the first order reaction rate law, the rate constant for each  $Cu/TiO_2$  was calculated and 2 wt%  $Cu/TiO_2$  has the highest rate constant ( $0.0574 \text{ min}^{-1}$ ). The photocatalyst loading and concentration loading were conducted. In photocatalyst loading study, 0.83 g/L of 2 wt%  $Cu/TiO_2$  can be concluded as the optimum weight loading for 300 mL of glycerol solution. In the glycerol solution study, the amount of photocatalyst (0.25g) considered not optimum to yield the maximum conversion.

## ABSTRAK

Beberapa jurnal telah mengemukakan tentang penghasilan  $H_2$  dari larutan gliserin dengan menggunakan pemangkin, salah satu cara yang inovatif ialah menggunakan photopemangkin. Dalam kajian ini, titania (Ti) menjadi sebagai tapak pemangkin dan copper (Cu) sebagai pendopan. Kajian ini bertujuan menghasilkan dan mentakrifkan sifat-sifat copper-titania ( $Cu/TiO_2$ ) untuk photoreaksi larutan gliserin.  $Cu/TiO_2$  dihasilkan dengan cara menperdopankan 2, 5, 10, 15, 20 dan 25 wt% Cu atas Ti. X-ray fluorescence (XRF) menunjukkan komposisi Cu mengikut peratusan pendopan atas Ti. Di samping itu, BET specific surface area menunjuk pengurangan dengan penambahan Cu. Thermogravimetric analysis (TGA) menunjukkan Cu mengurai dekat 450 hingga 550 K. X-ray diffraction (XRD) membuktikan  $Cu/TiO_2$  ialah anatase, puncak  $2\theta = 13^\circ$  ditemui dan puncak ini dipercayai sebagai kemunculan spesies CuO. Kepadatan  $Cu/TiO_2$  mengukur dengan gas pycnometer menunjukkan perbezaan dengan kepadatan teori. Photoreaksi  $Cu/TiO_2$  dicubakan dengan menggunakan methylene blue, reaksi methylene blue membuktikan pemangkin kajian ini berfungsi. 2 wt%  $Cu/TiO_2$  mempunyai reaksi yang paling tinggi dengan bacaan 97.78%. Walau bagaimanapun, reaksi ini menurun mengikut penambahan Cu kecuali pemangkin 25 wt%. Kadar pemalar setiap pemangkin dikirakan, 2 wt%  $Cu/TiO_2$  mempunyai kadar pemalar yang tertinggi,  $0.0574 \text{ min}^{-1}$ . Kajian ini diteruskan dengan tambahan berat pemangkin dan kepekatan larutan gliserin. Dalam kajian penambahan berat pemangkin, 0.83 g/L 2 wt%  $Cu/TiO_2$  mempunyai reaksi yang tertinggi. Dalam kajian penambahan kepekatan larutan gliserin, 100 mg/L larutan gliserin mempunyai reaksi yang terbaik.

## TABLE OF CONTENT

SUPERVISOR DECLARATION.....	II
DECLARATION .....	III
ACKNOWLEDGEMENTS .....	IV
ABSTRACT.....	V
ABSTRAK.....	VI
TABLE OF CONTENT.....	VII
LIST OF TABLES .....	IX
LIST OF FIGURES .....	X
LIST OF NOMECLATURES.....	XII
LIST OF ABBREVIATIONS.....	XIII
1 Introduction .....	1
1.1 Problem Statement .....	2
1.2 Objective .....	3
1.3 Scopes.....	3
2 Literature Review .....	4
2.1 Introduction .....	4
2.2 Glycerol.....	5
2.3 Physical and Chemical Properties .....	6
2.4 Photocatalyst .....	7
2.4.1 Mechanisms of Photocatalysis.....	9
2.4.2 Photocatalysis of Glycerol .....	11
2.5 Titanium Dioxide .....	14
2.5.1 Properties of Titanium Dioxide .....	14
2.5.2 Metal Doping on Titanium Dioxide.....	16
3 Methodology.....	23
3.1 Introduction .....	23
3.2 Chemicals .....	23
3.3 Photocatalyst Preparation .....	24

3.4	Photocatalyst Characterization .....	25
3.4.1	X-ray Fluorescence (XRF).....	25
3.4.2	X-ray Diffraction (XRD) .....	28
3.4.3	Liquid N <sub>2</sub> Physisorption (Brunauer-Emmett-Teller, BET) .....	29
3.4.4	Thermogravimetric Analysis (TGA).....	34
3.4.5	Gas Pycnometer .....	38
3.5	Photoreaction of Glycerol Solution.....	39
3.5.1	Chemical Oxygen Demand (COD).....	39
4	Results and Discussion .....	41
4.1	Introduction .....	41
4.2	Photocatalyst Characterization .....	41
4.2.1	Density Measurements.....	41
4.2.2	X-ray Fluorescence (XRF).....	43
4.2.3	X-ray Diffraction (XRD) .....	44
4.2.4	Liquid N <sub>2</sub> Physisorption (BET) .....	47
4.2.5	Thermogravimetric Analysis (TGA).....	49
4.3	Reactivity of Photocatalyst.....	51
4.4	Photoreaction of Glycerol Solution.....	52
4.4.1	Effects of Cu-metal Loading.....	52
4.4.2	Photoreaction Kinetic of Glycerol Solution.....	55
4.4.3	Effects of Catalyst Loading .....	58
4.4.4	Effects of Concentration Loading .....	59
5	Conclusions and Recommendations .....	61
5.1	Introduction .....	61
5.2	Conclusion.....	61
5.3	Recommendations .....	62
	REFERENCES .....	64
	Appendix A.....	69
	Appendix B .....	70
	Appendix C .....	90

## LIST OF TABLES

Table 2.1 Physical and chemical properties of related chemicals .....	7
Table 2.2 Typical physical and mechanical properties of TiO <sub>2</sub> .....	15
Table 2.3 TiO <sub>2</sub> under photocatalytic reaction with glycerol.....	18
Table 2.4 The physical properties of the TiO <sub>2</sub> and Cu/TiO <sub>2</sub> photocatalyst (Jeon et al., 2007) .....	22
Table 2.5 Generation of H <sub>2</sub> over TiO <sub>2</sub> and Cu/TiO <sub>2</sub> photocatalyst (Jeon et al., 2007) .....	22
Table 3.1 Lists of chemicals .....	24
Table 3.2 Lists of gases.....	24
Table 3.3 Process that lead to weight gain or loss in TGA experiments .....	35
Table 4.1 Density of Cu/TiO <sub>2</sub> photocatalyst .....	42
Table 4.2 Theoretical density of Cu/TiO <sub>2</sub> .....	42
Table 4.3 XRF characterization results.....	44
Table 4.4 Crystalline size of Cu.....	47
Table 4.5 BET results of freshly-calcined Cu/TiO <sub>2</sub> photocatalyst.....	48
Table 4.6 Pore volume and pore diameter of Cu/TiO <sub>2</sub> .....	49
Table 4.7 MB solution photoreaction results.....	52
Table 4.8 COD results from collected glycerol samples .....	53
Table 4.9 Rate constant, k of different loading Cu/TiO <sub>2</sub> .....	58
Table 4.10 Weight loading results and conversion for 2 wt% Cu/TiO <sub>2</sub> .....	59
Table 4.11 Concentration loading results and conversion of 2 wt% Cu/TiO <sub>2</sub> .....	60

## LIST OF FIGURES

Figure 2.1 Transesterification reaction of a triglyceride with ethanol, utilizing NaOH as a catalyst and rendering biodiesel and glycerol (Silva et al. 2009) .....	5
Figure 2.2 Structure of glycerol (Pachauri and He, 2006) .....	6
Figure 2.3 Schematic representation of a photoelectrochemical cell (PEC) (Fujishima and Tryk, 1999) .....	8
Figure 2.4 Photo absorption by a semiconductor causes electron transition from the valence band to the conduction band (Ohtani, 2010) .....	10
Figure 2.5 Fundamental principle of semiconductor's photocatalytic reaction (Chen et al., 2010) .....	10
Figure 2.6 Simplified mechanistic scheme showing the reaction occur over Pt/TiO <sub>2</sub> suspensions under conditions of water splitting (a + b); glycerol photo-reforming (a+ d); glycerol oxidation (c + d) (Panagiotopoulou et al., 2012) .....	12
Figure 2.7 Energy band gap of various semiconductors in aqueous electrolyte at pH = 1 (Yoong et al. 2009) .....	15
Figure 2.8 Crystal structures of (a) anatase, (b) rutile and (c) brookite (Carp et al., 2004) .....	16
Figure 2.9 Charge recombination and separation/migration processes on the surface of photocatalyst (Chen et al., 2010) .....	17
Figure 2.10 Diffuse reflectance spectra of TiO <sub>2</sub> catalyst with different Cu loading (wt%). The inset show the $(\alpha h\nu)^2$ versus $h\nu$ plots, where $\alpha$ is absorbance (Wu and Lee, 2004)..	19
Figure 2.11 Cu (2p <sub>3/2</sub> and 2p <sub>1/2</sub> ) XPS spectra of the catalysts subjected to (1) reduction, (2) H <sub>2</sub> production reaction, and (3) oxidation in air at room temperature for 120 h (Wu & Lee, 2004) .....	20
Figure 2.12 H <sub>2</sub> generation curve (Wu & Lee, 2004).....	21
Figure 2.13 SEM images of TiO <sub>2</sub> and Cu/TiO <sub>2</sub> after calcined at 500 °C and 800 °C (Jeon et al., 2007) .....	21
Figure 3.1 Schematic view of orbital transitions due to XRF.....	26
Figure 3.2 Diagram of a wavelength dispersive spectrometer (Jenkis, 1995) .....	27
Figure 3.3 A schematic diagram of XRD (A) Collimation (B) Sample (C) Slit (D) Exit Beam Monochromator (E) Detector (X) Source of X-Rays (Cullity, 1978) .....	29
Figure 3.4 Typical N <sub>2</sub> adsorption-desorption isotherms of mesoporous materials.....	31
Figure 3.5 Typical N <sub>2</sub> adsorption-desorption isotherms of large macroporous materials	32
Figure 3.6 Instrumentation flow diagram of TGA.....	36
Figure 3.7 Thermogram .....	36
Figure 3.8 Tangent curve to find onset and offset points .....	37

Figure 3.9 Typical TG curves .....	37
Figure 3.10 Helium gas displacement Pycnometer type 1305 Micromeritics .....	38
Figure 3.11 Photoreaction of glycerol solution.....	40
Figure 4.1 Comparison of densities from theoretical calculation and actual measurements .....	43
Figure 4.2 Complete XRD patterns for (a) 2wt% Cu/ TiO <sub>2</sub> (b) 5wt% Cu/ TiO <sub>2</sub> (c) 10wt% Cu/ TiO <sub>2</sub> (d) 15wt% Cu/ TiO <sub>2</sub> (e) 20 % Cu/ TiO <sub>2</sub> (f) 25wt% Cu/ TiO <sub>2</sub> .....	46
Figure 4.3 Typical adsorption/desorption isotherm for 2 wt% Cu/TiO <sub>2</sub> .....	48
Figure 4.4 20 wt% Cu/TiO <sub>2</sub> thermogram .....	50
Figure 4.5 Derivative weight profile of Cu/TiO <sub>2</sub> from 400 to 600 K .....	51
Figure 4.6 Fractional photo-conversion of glycerol solution over Cu/TiO <sub>2</sub> .....	54
Figure 4.7 Conversion and BET surface area trend line.....	55
Figure 4.8 Transient COD values during glycerol solution photo-decomposition with different active metal loadings.....	55
Figure 4.9 Plot of $\ln \frac{C_A}{C_{Ao}}$ versus time for 2-wt% Cu/TiO <sub>2</sub> .....	57
Figure 4.10 Complete graph of $\ln \frac{C_A}{C_{Ao}}$ as a function of t for different loading Cu/TiO <sub>2</sub> . ..	58



## LIST OF NOMECLATURES

Notation	Description
a	BET effective cross-sectional area
C	BET dimensionless constant
C	Concentration
d	Inter plane distance of crystal
D	Crystalline size (Å)
e <sup>-</sup>	Negative-electron
h <sup>+</sup>	Positive-hole
k	Rate constant (min <sup>-1</sup> )
k <sub>Sch</sub>	Scherrer constant
m	BET mass of solid catalyst
n	Order (interger)
N	Avogrado constant ( $6.022 \times 10^{23} \text{ mol}^{-1}$ )
P	BET partial vapor pressure
P <sub>a</sub>	BET ambient pressure
P <sub>o</sub>	BET saturated pressure
ppm	part per million (mg/L)
r	BET correlation coefficient
R	BET gas constant (8.314 E7 ergs/K.mol)
-r <sub>A</sub>	Photoreaction rate (mg/L.min)
r <sub>k</sub>	BET Kelvin radius of pore
r <sub>p</sub>	BET actual pore radius
S	BET specific surface area
T	BET ambient temperature
t	time
V <sub>a</sub>	BET volume of gas adsorbed at STP
V <sub>ads</sub>	BET volume of N <sub>2</sub> adsorbed
V <sub>liq</sub>	BET volume of liquid
V <sub>m</sub>	BET volume of gas absorbed at STP to monolayer coverage
w	Weight fraction
wt%	Weight percent
X	Conversion
β <sub>d</sub>	Angular width of half-maximum intensity (degree/°)
γ	BET surface tension of N <sub>2</sub> (8.85 ergs.cm <sup>2</sup> at 77.4 K)
θ	Angle (degree/°)
λ	Wavelength (nm)
ρ	Density

**LIST OF ABBREVIATIONS**

---

BET	Brunauer-Emmett-Teller
BJH	Barrett, Joyner and Halenda
BOD	Chemical oxygen demand
COD	Biochemical oxygen demand
DH	Dollimore and heal
ED	Energy-dispersive
MB	Methylene blue
STP	Standard temperature and pressure
TGA	Thermogravimetric analysis
UMP	Universiti Malaysia Pahang
UV	Ultraviolet
UV-Vis	Ultraviolet-visible spectrometer
WD	Wavelength-dispersive
XRD	X-ray diffraction
XRF	X-ray fluorescence

---

## **CHAPTER 1**

### **INTRODUCTION**

#### **1 Introduction**

The current global economy is largely dependent on fossil fuels, from heavy industries to transportation and daily life goods production. The indiscriminate burning of fossil fuels however has led to environmental degradation. Moreover, these fossil hydrocarbon sources are not renewable. Hence, a suitable alternative and renewable energy sources such as hydrogen is fast gaining attention from the researchers (Yoong et al., 2009). According to Das and Veziroglu (2001), hydrogen is the most plentiful element in the universal, representing about three-quarters of all the matter. Significantly, during the hydrogen combustion, water is the only product being generated. Therefore, compared to other fuels as per se, hydrogen is perceived as a non-polluting fuel and proven to be harmless to humans and environment.

In the year 2011 alone, National Biodiesel Board (NBB) reported production of more than 802 million gallons of biodiesel far superseding 2010 production of just 315 million gallons. From chemical perspective, biodiesel is defined as the mono-alkyl esters of long chain fatty acid derived from reaction between vegetable oils or animal fats with alcohol in the presence of or without a catalyst (Atanani et al., 2012). According to

Leoneti et al. (2012), biodiesel production process involves transesterification process, with generation of glycerol by-product. During this reaction, roughly 10% of the feedstock is converted into glycerol (Abad & Turon, 2012). Nonetheless, the burgeoning diesel industry creates a glut of glycerol as a potential industrial waste due to the lack of the supporting industries (Slamet et al., 2011).

For the past few years, most of the research scopes focused on crude glycerol utilization in particular for conversion into valuable product; in fact several papers have addressed the production of hydrogen from glycerol solution using catalyst (Skaf et al., 2012). According to Melo and Silva (2011), the on-going research has discovered different methods to produce hydrogen from glycerol such as steam reforming, gastification, autothermal reforming, aqueous-phase reforming, electrochemical reforming, photofermentation and supercritical water reforming processes. All these studies were related to thermochemical routes. However, hydrogen can be produced from biomass in ambient conditions (temperature and pressure) via a photocatalytic route, an efficient, ecologically benign and low-cost process which based on photochemical cells operating with two redox system.

## **1.1 Problem Statement**

The continuous production of biodiesel as future transportation fuel is anticipated to increase the glycerol production. In Malaysia, glycerol is classified as a waste under Schedule S181 of the Environmental Regulations and stored in drums before subsequently disposed in landfills (Hidawati & Sakinah, 2011). In addition, Kualiti Alam Waste Management Centre is the only statutory body handling these scheduled wastes where disposal and its treatment are carried out at prescribed premises only with a certain amount of charges imposed for every tonne of waste disposal. The cost for landfill is approximately RM 500 while incineration costs around RM 810/t to RM 3600/t (Hazimah et al., 2003).

Moreover, the amount of glycerol generated significantly increase because the biodiesel market is being expanded around the world, this lead to the problem of the surplus of glycerol in the market (Sreethawong et al., 2011). According to Varrone et al.

(2012), the considerable growth of the biodiesel industry has depressed the price of crude glycerol; this decrease in price poses a problem for the glycerol-producing and -refining industries, and the economic viability of the biodiesel industry itself has been greatly affected. Therefore, the development of processes to convert low-value glycerol into higher value products is expected to the development of biorefineries and also adds value to the production of biodiesel (Dharmadi et al., 2006).

## **1.2 Objective**

The objective of this research work is to synthesize and to study the physicochemical properties of Cu/TiO<sub>2</sub> photocatalyst for the photoreaction of glycerol solution.

## **1.3 Scopes**

In order to achieve the objectives of the current work, the following scopes have been identified:

- I. To synthesize Cu/TiO<sub>2</sub> photocatalyst using wet impregnation method with the dopant metal loadings ranged from 2, 5, 10, 15, 20 and 25 wt%.
- II. To characterize the physicochemical properties of Cu/TiO<sub>2</sub> photocatalyst using spectroscopic analyses such as:
  - a) X-ray fluorescence (XRF)
  - b) Liquid-nitrogen physisorption (Brunauer-Emmett-Teller, BET)
  - c) X-ray diffraction (XRD)
  - d) Thermogravimetric analysis (TGA)
  - e) Gas pycnometer
- III. To study the effect of different metal loadings of Cu/TiO<sub>2</sub> photocatalyst on the photoreaction of glycerol solution.

## **CHAPTER 2**

### **LITERATURE REVIEW**

## **2 Literature Review**

### **2.1 Introduction**

The demand for cleaner industrial processes and sustainable energy production from renewable source is growing as a consequence of higher public awareness towards environmental preservation (Gombac et al., 2010). According to Yoong et al. (2009), hydrogen ( $H_2$ ) is classified as the future energy because it is renewable, does not emit “greenhouse gas” carbon dioxide during oxidation, possesses large specific energy density and easily convertible to electricity by fuel cells. In the current energy scenario, an approximately 95% of  $H_2$  consumed is derived from fossil fuels via catalytic thermal and gasification routes at elevated temperature (Slamet et al., 2011). Numerous methods have been proposed to produce hydrogen from renewable sources. Nevertheless, sustainable hydrogen production from solar photocatalytic splitting of water remains an ultimately challenging dream (Gombac et al., 2011). In contrast, photocatalytic hydrogen generation from glycerol has begun to gain attention from researchers in lieu of growing demand of biodiesel as liquid transportation fuel; hence generation of glycerol as by-product during transesterification.

## 2.2 Glycerol

Glycerol is a widely utilized ingredient in the production of cosmetic, paint, automotive, food tobacco, pharmaceutical, pulp and paper, leather and textile industries and even as feedstock for the production of various chemicals. Glycerol was produced commercially via fermentation route for the first time using the sulfite-steered yeast process during World War I, when the demand for glycerol in explosive manufacture exceeded the supply from the soap industry (Prescott & Dunn, 1959). According to Wang et al. (2001), glycerol is released as a by-product during the hydrolysis of fats but this process is currently less important because the soap production is now replaced by detergents.

In particular, the global demand for biofuels is currently on the rise worldwide and the use of biomass as one of the most promising alternatives has amplified its amount. According to Silva et al. (2008), one of the biofuel which originated from biomass is biodiesel. It is mainly produced from the vegetable oils and animal fats. Significantly, it can be blended with the petroleum based diesel in diesel engine motor. Glycerol is the by-product obtained during transesterification of vegetable oils and animal fats as shown in Figure 2.1 (Solomon et al., 1995).

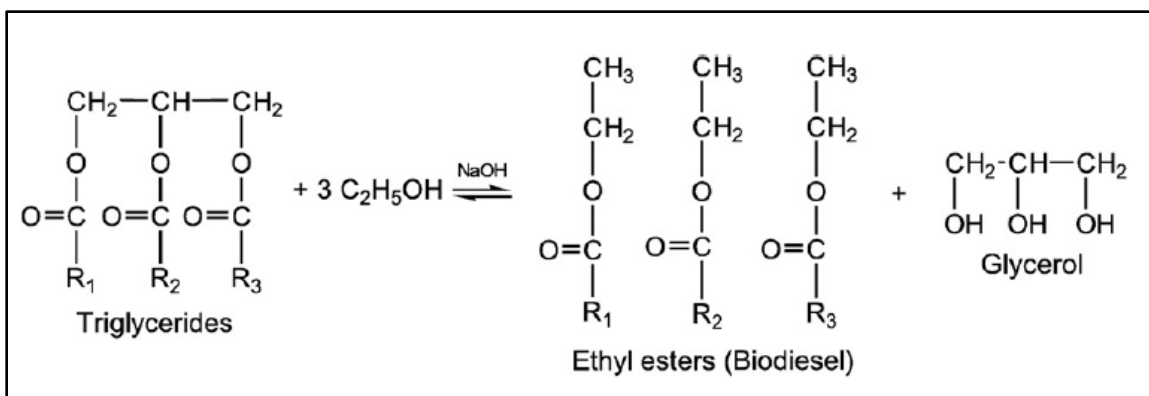


**Figure 2.1** Transesterification reaction of a triglyceride with ethanol, utilizing NaOH as a catalyst and rendering biodiesel and glycerol (Silva et al. 2009)

According to Dasari et al. (2005), for every 9 kg of biodiesel produced, about 1 kg of a glycerol by-product is formed. Hence, the effective usage or conversion of glycerol will reduce the biodiesel production costs (Pachauri & He, 2006).

In terms of chemical structure, glycerol (also known as 1,2,3-propanetriol, glycerine, glycerin, glycylic alcohol, cf. Figure 2.2) is a trihydric alcohol. In addition, it is a colourless, odourless, and sweet-tasting, syrupy liquid at ambient condition with molecular weight of 92.09. It is generally known that crude glycerol has a purity of 70 to 80% and is often concentrated and purified to commercial sale, ranging from 95.9 to 99% purity (water is the impurity) before sale. It melts at 290.8 K and boils with decomposition at 563 K. Furthermore, glycerol is completely soluble in water and alcohol, slightly soluble in ether, ethyl acetate and dioxane; and insoluble in hydrocarbons. Moreover, it is highly stable under normal storage conditions, non-irritating and has no known negative environmental effects. Glycerol contains three hydrophilic alcoholic hydroxyl groups attached to the hydrocarbon backbone. This polar group is responsible for its solubility in water and hygroscopic behaviour. It is a highly flexible molecule forming both intra- and intermolecular hydrogen bonds (Pagliaro & Rossi, 2008).

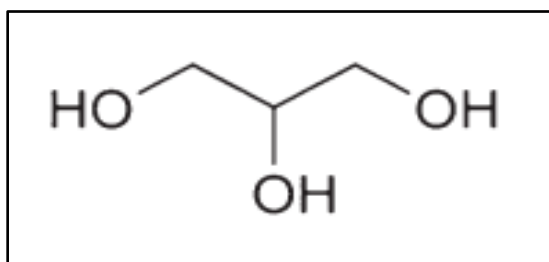


**Figure 2.2** Structure of glycerol (Pachauri and He, 2006)

### 2.3 Physical and Chemical Properties

Table 2.1 lists the physical and chemical properties of the chemical compounds (solid, liquid and gas phases) partake in glycerol photocatalysis.



**Table 2.1** Physical and chemical properties of related chemicals

Chemical	Function	Physical and Chemical Properties
Glycerol (C <sub>3</sub> H <sub>8</sub> O <sub>3</sub> )	Reactant	<ul style="list-style-type: none"> <li>• Form: Viscous colourless liquid</li> <li>• Molecular weight: 92.09</li> <li>• Melting point: 290.8 K</li> <li>• Boiling point: 563 K</li> <li>• Solubility: complete soluble in water and alcohol; insoluble in hydrocarbon</li> </ul>
Titanium dioxide (TiO <sub>2</sub> )	Photocatalyst	<ul style="list-style-type: none"> <li>• Form: White crystalline solid</li> <li>• Molecular weight: 79.87</li> <li>• Melting point: 2073 K</li> </ul>
Copper (Cu)	Photocatalyst	<ul style="list-style-type: none"> <li>• Form: Reddish metal</li> <li>• Atomic weight: 63.55</li> <li>• Melting point: 1357.62 K</li> <li>• Boiling point: 2835 K</li> <li>• Moderately active metal, dissolves in most acids and in alkalis</li> </ul>
Titanium (Ti)	Photocatalyst	<ul style="list-style-type: none"> <li>• Form: White metal</li> <li>• Atomic weight: 47.88</li> <li>• Melting point: 1933 K</li> <li>• Boiling point: 3560 K</li> <li>• Non-reactive, more reactive in high temperature</li> <li>• Resists corrosion</li> </ul>
Carbon dioxide (CO <sub>2</sub> )	Product	<ul style="list-style-type: none"> <li>• Form: Colourless, odourless gas</li> <li>• Molecular weight: 44.01</li> <li>• Freezing point: 194.5 K</li> </ul>
Hydrogen (H <sub>2</sub> )	Product	<ul style="list-style-type: none"> <li>• Form: Colourless, odourless gas</li> <li>• Atomic weight: 2.0159</li> <li>• Melting point: 13.9 K</li> <li>• Boiling point: 20.12 K</li> <li>• Burns in air or oxygen to produce water.</li> <li>• Combine readily with non-metals and halogens</li> </ul>

## 2.4 Photocatalyst

The photo-electrochemical splitting of water was first reported in 1972 by Fujishima and Honda. This discovery attracted world-wide attention and triggered enormous research activity in numerous laboratories, post oil-crisis in 1973. Concerted efforts are underway to find semiconductors that utilize the solar spectrum in an effective

way to photo-split water. Figure 2.3 shows the first photo-electrochemical cell that was constructed for the water decomposition water into hydrogen and oxygen.

When UV light irradiated the surface of the  $\text{TiO}_2$ , a water oxidation reaction will occur and oxygen is produced at the  $\text{TiO}_2$  electrode. Concomitant reduction then will lead to hydrogen production at the platinum (Pt) black electrode. This indicates that water ( $\text{H}_2\text{O}$ ) can be decomposed into  $\text{O}_2$  and  $\text{H}_2$  using UV light without the application of an external voltage (Fujishima et al., 2000).

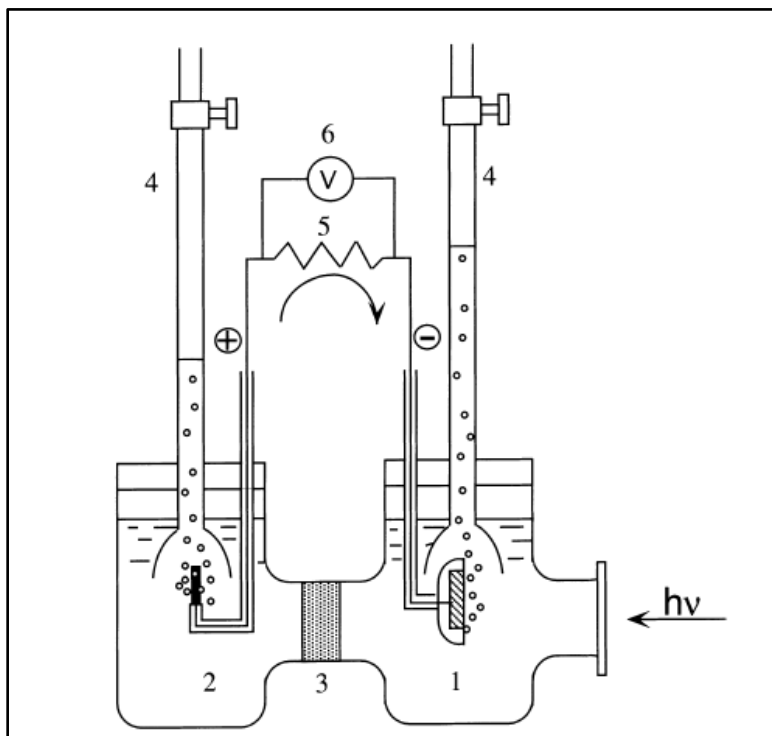
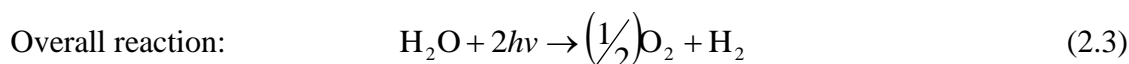
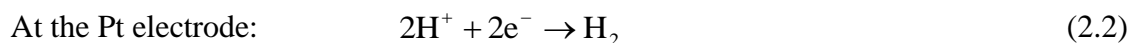
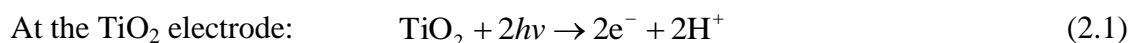


**Figure 2.3** Schematic representation of a photoelectrochemical cell (PEC) (Fujishima and Tryk, 1999)

Where,

- (1) n-type  $\text{TiO}_2$  electrode
- (2) Platinum black counter electrode
- (3) Ionically conducting separator
- (4) Gas burette
- (5) Load resistance
- (6) Voltmeter

Photocatalytic reaction can be simply defined as the excitation of a solid semiconductor by UV-visible light, generating free electrons and holes that partake in redox process on the catalyst surface and the attack of absorbed molecules (Bouchy & Zahraa, 2003). This concept was later applied by Bard (1982) to the design of a photocatalytic system using semiconductor particles or powders as photocatalyst.

#### **2.4.1 Mechanisms of Photocatalysis**

According to Carp et al. (2004), photocatalytic process can be described as the light-induced excitation of semiconductor. The light source supplies higher energy than the material band gap energy. Consequently, an energy-rich electron-hole pair is formed as illustrated in Figure 2.4.

When a photocatalyst absorbs UV or visible light, the electrons in the valence band of the photocatalyst are excited to the conduction band. As a result, the negative-electron ( $e^-$ ) and positive-hole ( $h^+$ ) pairs are created as reducing and oxidizing agents. At this stage, it is called as semiconductor's "photo-excited" and the energy difference between the valence band and conduction band is termed as "band gap" as shown in Figure 2.5.

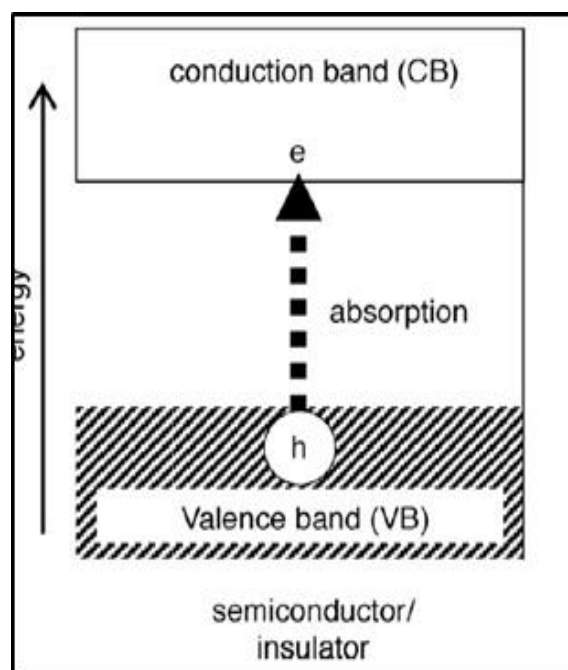


**Figure 2.4** Photo absorption by a semiconductor causes electron transition from the valence band to the conduction band (Ohtani, 2010)

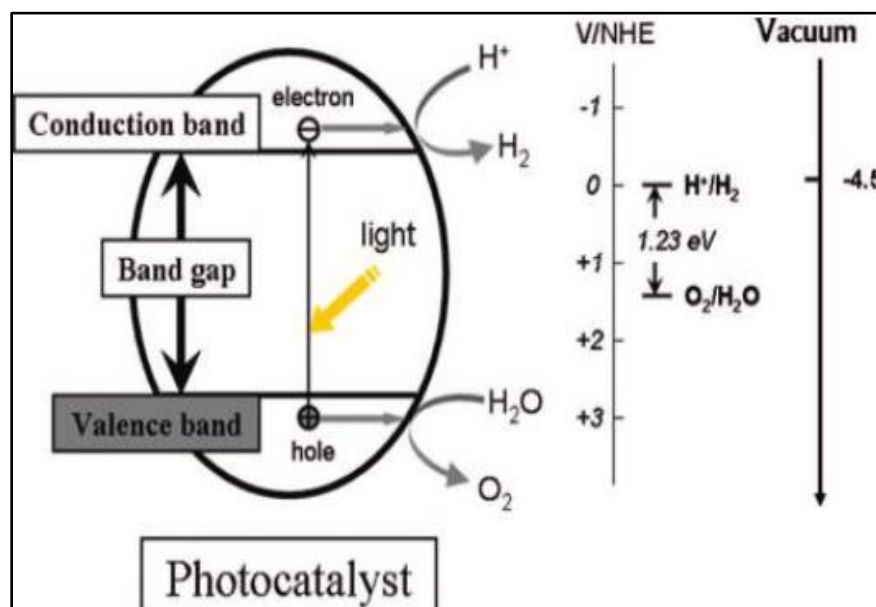
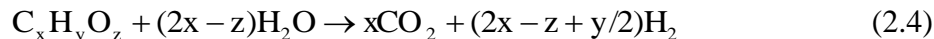


**Figure 2.5** Fundamental principle of semiconductor's photocatalytic reaction (Chen et al., 2010)

### 2.4.2 Photocatalysis of Glycerol

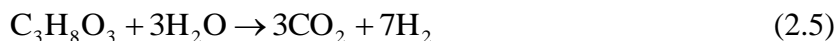
Kondarides et al. (2008) had tested a large variety of biomass-derived components including monosaccharide such as pentoses (ribose, arabinose) and hexoses (glucose, galactose, fructose and mannose), alcohols (methanol, ethanol, propanol and butanol) and organic acids (acetic acid, formic acid). From their studies, they have concluded that the amounts of  $H_2$  and  $CO_2$  produced were represented by the Equation (2.4):



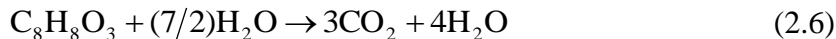
Daskalaki and Kondarides (2009) furthered the study on photo-reforming of glycerol with the use of Pt/TiO<sub>2</sub> as photocatalyst under UV light irradiation. They found that  $H_2$  can be produced efficiently by the photocatalytic reforming of aqueous glycerol solution and it showed complete conversion of glycerol to  $H_2$  and  $CO_2$ .

According to Panagiotopoulou et al. (2012), the overall photo-reforming reaction of organic compounds can be described as the combination of water reduction and oxidation of the organic substrate into a single process that is able to produce  $H_2$  at room temperature and atmospheric pressure. In their study, they made the comparison between the kinetic and mechanism of the glycerol photo-reforming and photo-oxidation reaction of glycerol over Pt/TiO<sub>2</sub> as photocatalyst.

For glycerol photo-reforming, the reaction can be shown as in Equation (2.5):



For glycerol photo-oxidation, the reaction can be shown as in Equation (2.6):



In the presence of  $O_2$ , glycerol is oxidized towards  $CO_2$  by valence band holes (cf. Figure 2.6 (d)); while the conduction band electrons reduce  $O_2$  to produce additional oxidizing species (Figure 2.6 (c)). Photo-reforming reaction typically takes place under unaerated conditions. Therefore, photogenerated holes are utilized to oxidize the organic compound (Figure 2.6 (a)) and the electrons are free to reduce water towards hydrogen (cf. Figure 2.6 (d)). Significantly, the hydrogen generation rate under photo-reforming is

comparatively higher than photocatalytic by water photo-splitting attributed to the efficient scavenging of the photogeneration by the organic substrate.

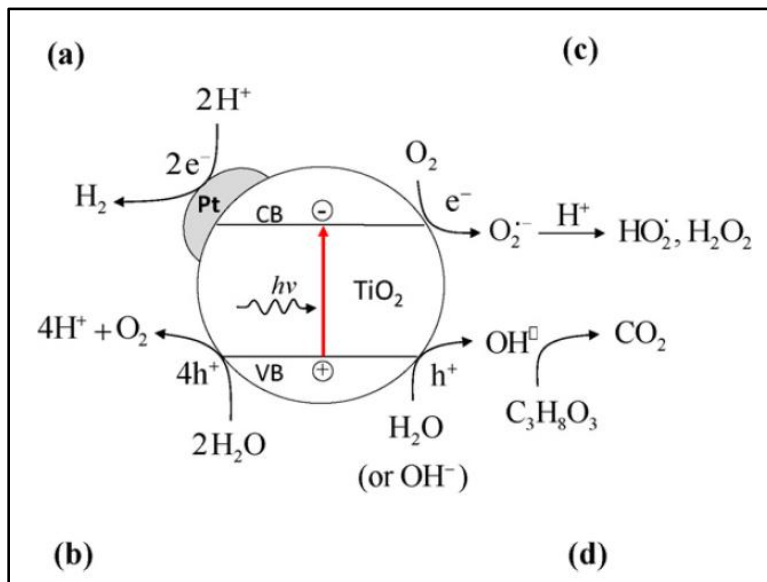
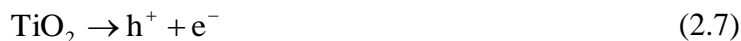


**Figure 2.6** Simplified mechanistic scheme showing the reaction occur over Pt/TiO<sub>2</sub> suspensions under conditions of water splitting (a + b); glycerol photo-reforming (a+ d); glycerol oxidation (c + d) (Panagiotopoulou et al., 2012)

According to Li et al. (2009), the complete mechanism of glycerol photo-reforming can be surmised as following (2.7) to (2.6). Firstly, the light results in the intrinsic ionization of semiconduction material (TiO<sub>2</sub>) over the band gap, leading the formation of h<sup>+</sup> and e<sup>-</sup>, then the light induced holes split water into hydroxide ions and hydrogen ions. Simultaneously, the electron generated reduces the hydrogen ions to H<sub>2</sub> gas.





Glycerol absorbed on the catalyst reacted and formed hydroxyl radical:



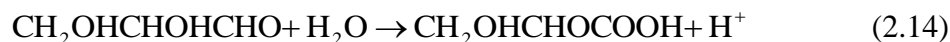
Thereafter, the  $\text{CH}_2\text{OHCHOHCHOH}$  species reacts with water to form  $\text{CH}_2\text{OHCHOHCH}(\text{OH})_2$  species and  $\text{H}^+$  ion to produce  $\text{H}_2$ .



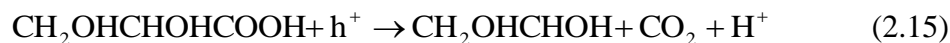
The  $\text{CH}_2\text{OHCHOHCH}(\text{OH})_2$  species is unstable, then transformed into aldehyde:



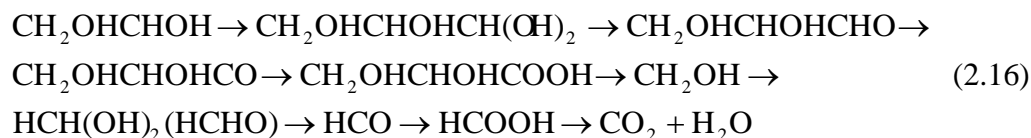
$\cdot\text{OH}$  species then reacts continuously with the aldehyde:



Decarboxylation occurs when the  $\text{CH}_2\text{OHCHOHCOOH}$  species reacts with photo-induced hole ( $\text{h}^+$ ).



The  $\text{CH}_2\text{OHCHOH}$  formed repeats the aforementioned reaction until finally form  $\text{H}_2\text{O}$  and  $\text{CO}_2$ .



## 2.5 Titanium Dioxide

Titanium is the world's fourth most abundant metal after aluminium, iron and magnesium; and the ninth most abundant element which constitutes about 0.63% of the earth crust. It was discovered by Reverend William Gregor in 1791 in England. According to Carp et al. (2004), titanium metal is not found unbound to other elements but occurs primarily in minerals like rutile, ilmenite, leucoxene, anatase, brookite, perovskite, sphene and also found in titanates and many iron ores.

Titanium dioxide or titania ( $\text{TiO}_2$ ) is the transition metal oxides.  $\text{TiO}_2$  started replacing toxic lead oxides as pigments for white paint industrial since the beginning of the 20<sup>th</sup> century and the annual production of  $\text{TiO}_2$  exceeds 4 million tons (Greenwood et al., 1997; Natara et al., 1998). Overall, approximately 51% of  $\text{TiO}_2$  production is used as a white pigment in paints, 19% in plastic, 17% in paper and others in minor sector.

### 2.5.1 Properties of Titanium Dioxide

As compared with other semiconductors (cf. Figure 2.7),  $\text{TiO}_2$  is considered as a good photocatalyst for hydrogen generation because of its stability.  $\text{TiO}_2$  can only absorb photon near UV-range with 380 nm or less due to its large band gap of 3.2 eV. Consequently the  $e^-$  can only be excited in this UV-range (Tang et al., 2012).

According to Yoong et al. (2009), the use of UV radiation alone for photocatalytic reaction is not an economically option, it is a must to shift the edge of adsorption of Hence, many efforts have been made to extend the optical response of  $\text{TiO}_2$  from UV-range to visible light range (400 – 750 nm). Unfortunately, there is limit in the research associated with visible light range. Melo and Silva (2011) have mentioned that many efforts have been commenced to extend the optical response of  $\text{TiO}_2$  towards the visible region in order to fully harvest solar energy, since it accounts for approximately 43% of the incoming solar energy spectrum.